J Electr Eng Technol.2018; 13(3): 1138-1146
http://doi.org/10.5370/JEET.2018.13.3.1138

ISSN(Print) 1975-0102
ISSN(Online) 2093-7423

Performance Comparison of Conventional and Segmental Rotor Type Switched Reluctance Motor

Kwang-Il Jeong*, Zhenyao Xu, Dong-Hee Lee* and Jin-Woo Ahn†**

Abstract – Performance comparisons of switched reluctance motor for cooling fan application are dealt in this paper. Conventional and novel segmental type motors with the same dimension are compared. The conventional 12/8 type is very popular and used widely. The structure of segmental rotor type motor is constructed from a series of discrete segments, and the stator is constructed from two types of stator poles: exciting and auxiliary poles. This type of motor has short flux path and no flux reversal in the stator. The auxiliary poles are not wound by the windings and only provide the flux return path. Compared with conventional SRM, the segmental structure increases electrical utilization of the machine and decreases core losses, which leads to higher efficiency. To verify the segmental structure, finite element method (FEM) is employed to get static and dynamic characteristics of both SRMs. Finally, the prototypes of conventional and segmental SRMs are tested for characteristics comparisons.

Keywords: Reluctance motor, Segmental rotor, Short flux path, High efficiency.

1. Introduction

Switched Reluctance Motor (SRM) is a doubly-salient and singly-excited machine wherein the stator carries the winding and the rotor is simply made of stacked silicon steel laminations. Compared with the other types of motors, an SRM has several advantages, such as: less maintenance, higher fault tolerance, rugged construction, no permanent magnet, simple structure and very wide range of speed [1-4]. Furthermore, SRM has several outstanding characteristics, such as good reliability and lower hysteresis loss [2-6]. With these advantages, the SRM has gained more attention recently and has been treated as a good alternative for the electric motor drive application. In contrast, the SRM possesses several disadvantages, including torque ripples, which are produced in SRM because of its operating principle and magnetic structure. The torque ripples contribute to mechanical wear and acoustic noise. These torque ripples can be reduced, and the performance of the SRM can be improved by modifying the geometry or by using an appropriate control method. The optimal control method to reduce the torque ripple is not discussed in this paper. Nowadays, full pitch windings are used in SRMs to increase the electrical utilization of the machine, which improves torque capability at the expense of an increased end-winding length [7-9].

In this paper, performance comparisons of switched reluctance motor for cooling fan application are dealt, and a novel 12/8 segmental type SRM with short flux path and no flux reversal in the stator is proposed [10]. Unlike conventional structures, the rotor of the proposed structure is constructed from a series of discrete segments and the stator is constructed from two types of stator poles: exciting and auxiliary poles, in which the segmental core is embedded in aluminum (conductive metal) rotor block in order to increase the mechanical strength and easy manufacturing as well as to improve the torque performance. Compared with conventional SRM, the segmental structure increases the electrical utilization of the machine, decreases the magnetomotive force (MMF) requirements and core losses. All characteristics of conventional and segmental SRMs are analyzed by FEM and experiments.

2. Concept of Conventional and Segmental SRMs

This section presents the basic principles of conventional and segmental SRMs. Furthermore, in order to show the advantages of the segmental structure, the flux path of conventional and segmental SRMs in the stator during motor's commutation will be explained.

2.1 Conventional 12/8 SRM

Fig. 1 shows a typical structure of a conventional 3-phase 12/8 SRM with Phase A at aligned position. As shown in the figure, at this position, when Phase B is excited, the rotor will rotate in clockwise direction and when Phase C is excited, the rotor will rotate in counterclockwise direction. So, the rotor can rotate clockwise or counterclockwise according to the excitation sequence. Fig. 2 (a), (b) and (c)

† Corresponding Author: Dept. of Mechatronics Engineering, Kyungsung University, Korea. (jwahn@ks.ac.kr)
* Dept. of Mechatronics Engineering, Kyungsung University, Korea. (you486-7179@hanmail.net, leedh@ks.ac.kr)
** Shenyang Institute of Automation, China. (zhenyao87@163.com)
Received: June 28, 2016; Accepted: October 20, 2017

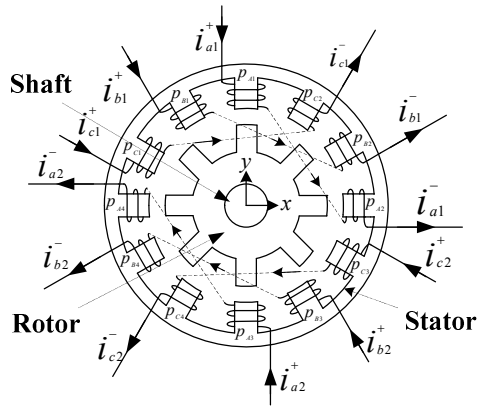

Fig. 1. Conventional 12/8 SRM

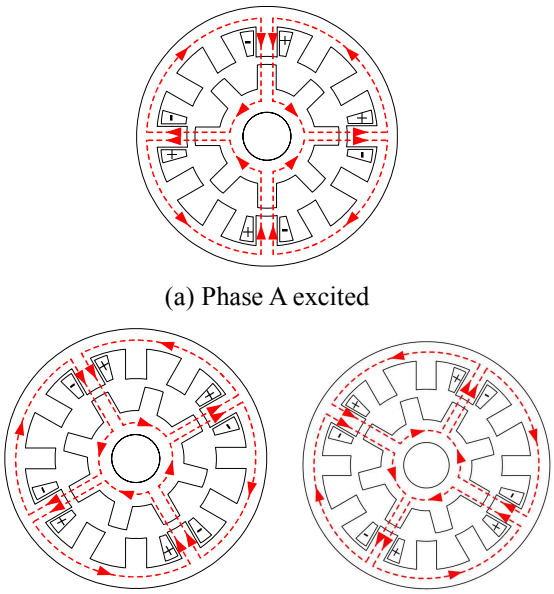

(a) Phase A excited

(b) Phase B excited (c) Phase C excited

Fig. 2. Flux paths in conventional 12/8 SRM

show the magnetic flux path of 12/8 SRM with rotor rotating in clockwise direction. In this figure, "-" stands for the current flow into the paper, and "+" stands for the current flow out the paper. When the phase current changes from Phase A to B, it has one-third flux reversal in the stator yoke and one-half flux reversal in the rotor yoke. The phenomenon is the same when the phase current changes from Phase B to C. Therefore, the core loss is almost the same in these two commutation regions. However, when the phase current changes from Phase C to A, it will be a little different from the current changing from Phase A to B, or Phase B to C, since there will be two-thirds flux reversal in the stator yoke and one-half flux reversal in the rotor yoke. Because the length of flux reversal path is increased, the core loss is also increased in this commutation region compared with the other two commutation regions. In order to increases the electrical utilization of the machine and decreases the core losses, a

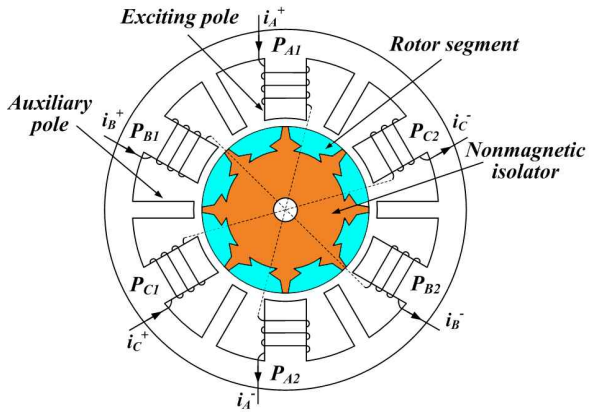

Fig. 3. Proposed 12/8 SRM

novel 12/8 segmental rotor type SRM is proposed in this paper.

2.2 Novel 12/8 segmental rotor type SRM

The concept of the proposed motor is based on the conventional 12/8 3-phase SRM. The 12/8 SRM employs a long magnetic flux path. This magnetic path is related to the core loss of a motor. A short magnetic path is better than the long one to reduce MMF. To realize a short magnetic path in the 3-phase motor, the stator-rotor poles of a 12/8 motor needs to be modified. The stator poles should be able to stream the magnetic flux through the shortest path, while the rotor poles should be able to drain the magnetic flux in any rotor position. The modified structure makes the conventional 12/8 SRM into a 12/8 segmental rotor type SRM with short flux path and no flux reversal in the stator. The concept of the proposed 3-phase 12/8 segmental rotor type SRM is proposed in Fig. 3. Unlike conventional structures, the rotor is constructed from a series of discrete segments where each rotor is embedded in aluminum rotor block and magnetically isolated from its neighbors. From Fig. 3, it can be seen that the stator has two types of stator poles: exciting and auxiliary poles. The exciting poles are wound by the windings, while the auxiliary poles are not wound by the windings and only provide the flux return path. Windings on the exciting poles P_{A1} and P_{A2} are connected in series to construct Phase A, windings on the exciting poles P_{B1} and P_{B2} are connected in series to construct Phase B, and windings on the exciting poles P_{C1} and P_{C2} are connected in series to construct Phase C. A short magnetic flux path can be achieved by incorporating one exciting and two adjacent auxiliary poles into one magnetic circuit. The advantages of a short magnetic flux are the ability to increase the efficiency and torque production while decreasing the core loss. Fig. 4(a) shows the magnetic paths of the proposed structure when phase A is excited at the aligned position. The magnetic paths of proposed structure with phase B and C energized are shown in Fig. 4(b) and (c), respectively. As

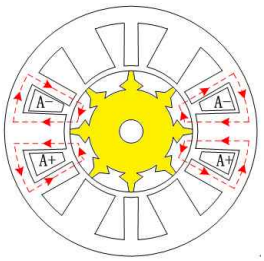

(a) Phase A excited

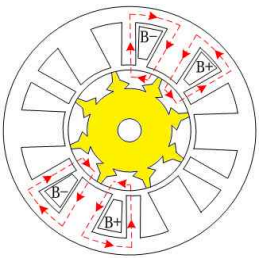

(b) Phase B excited

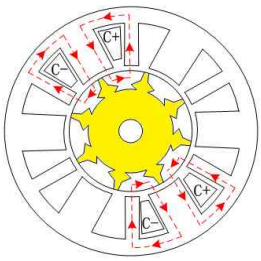

(c) Phase C excited

Fig. 4. Flux paths in the proposed 12/8 SRM

shown in the figures, the magnetic flux flows down from the exciting pole, through the rotor segments and returns via the adjacent auxiliary poles. All conductors in each slot only couple with the flux driven by their own MMF with very little mutual coupling between one slot and another, which increases the electrical utilization of the machine and decreases the MMF requirement. Meanwhile, in the segmental structure, short flux paths are taken and no flux reversal exists in the yoke side of the stator, which may lead to lower core losses.

2.3 Design of Conventional and Segmental SRMs

To verify the segmental structure, a prototype of the novel structure is designed for comparison with a conventional 12/8 SRM, which is designed for cooling fan application (12V, 500W, and 2800rpm). The following assumptions are made to enable this comparison.

a) The SRMs are designed for the same application so that the external stator dimensions and shaft diameters are the same. The stack lengths are also equal so that the both machines roughly have the same volume.
b) The wire gauge is the same to keep the same conductivity.
c) The flux density should be kept lower than 1.8 Tesla to satisfy the actual material requirement.
d) The slot factor should be kept the same or lower than 12/8 SRM.

The assumptions are reasonable design criteria that can be used to compare the two machines. Table 1 shows the detailed parameters of both SRMs. The prototypes of conventional and segmental type 12/8 SRM are manufactured, as shown in Fig. 5 and 6.

The materials of both motors are same, the stator and rotor lamination of the designed machine are S18, and the rotor block and shaft are brass BS2 grade and S45C, respectively. The main specifications of the prototype motors are shown in Table 1.

Table 1. Parameters of conventional and segmental type SRM

Parameter	Conventional SRM	Segmental SRM
Number of phase	3	3
Outer radius (mm)	52.5	52.5
Outer radius of rotor (mm)	31	28
Length of air gap (mm)	0.30	0.30
Inner radius of rotor (mm)	24	—
Radius of shaft (mm)	4	4
Stator tooth width (mm)	7.6	14.5/5.6
Stator pole arc (°)	14	30/12
Rotor pole arc (°)	16	41
Resistance per phase (mΩ)	7	6.7

(a) Rotor (b) Stator with windings

Fig. 5. Prototype of conventional 12/8 SRM

(a) Rotor (b) Stator with windings

Fig. 6. Prototype of segmental 12/8 SRM

3. FEM Analysis and Experimental Results

SRM has very high nonlinear magnetization characteristics. Hence, to verify the segmental structure, finite element method (FEM) is employed to get the characteristics of conventional and segmental type SRMs.

3.1 Static characteristics

3.1.1 Magnetic flux density

SRM is normally designed to operate in the saturated region. Figs. 7 and 8 show the flux density of conventional and segmental rotor type SRMs, when the motors operate in the full load condition (peak excitation current is 110 A).

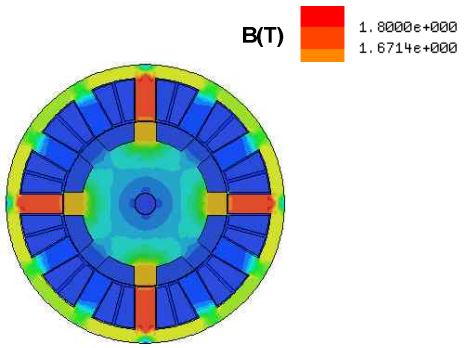

Fig. 7. Magnetic flux density of conventional 12/8 SRM

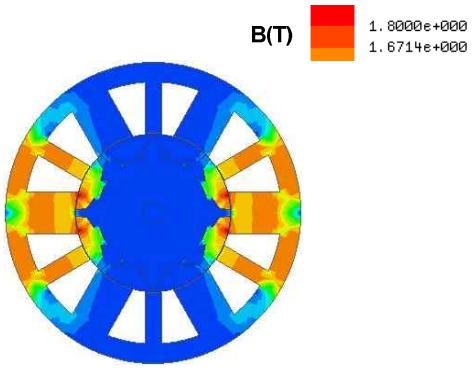

Fig. 8. Magnetic flux density of segmental 12/8 SRM

As shown in the figures, the maximum flux density in both structures are almost the same and less than 1.8 T, which satisfies the design requirements.

3.1.2 Inductance characteristics

The inductance profile has a considerable effect on the motor operation and is also related to the torque production.

The aligned position of a phase is defined to be the orientation when the stator and rotor poles of the phase are fully aligned, attaining the minimum reluctance position. The phase inductance is maximized in this position. Phase inductance decreases gradually as the rotor poles move away from the aligned position in either direction. When the rotor poles are symmetrically misaligned with the stator poles of a phase, the position is said to be the unaligned position, and the inductance is minimized in this position. In most SRM applications, saturation results in nonlinear inductance. Since the conventional 12/8 and segmental SRM have eight rotor poles, a rotation of 22.5°, from alignment to nonalignment, is sufficient to obtain the inductance characteristics of one electrical cycle.

Assume that the initial rotor position is at the fully aligned position and the rotor rotates in the counter-clockwise direction. In the case of the aligned stator-rotor position (0° and 45°), the inductance is at its highest and the magnetic reluctance of the flux is at its lowest. The inductance curves of both SRMs with respect to the rotor position are shown in Fig. 9.

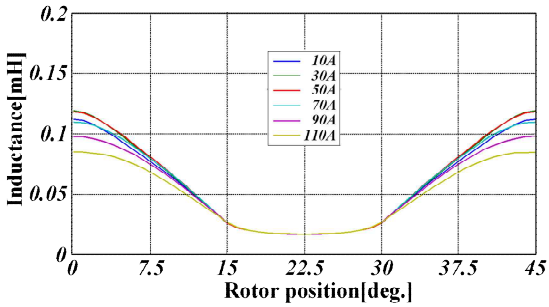

(a) Conventional SRM

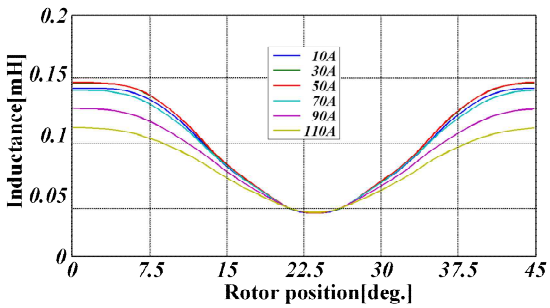

(b) Segmental SRM

Fig. 9. Inductance profiles at all current levels

Table 2. Inductance of conventional and segmental type SRM

Parameter	Conventional	Segmental
Maximum inductance (mH)	0.085	0.122
Minimum inductance (mH)	0.022	0.047
Rate d$L(\theta, i)$/dθ (mH/deg)	0.0028	0.0033

The torque T of an SRM, which is related to the rotor position (θ) and phase current (i), can be expressed as:

$$T = \frac{1}{2} i^2 \frac{dL(\theta,i)}{d\theta} \tag{1}$$

From (1), it can be seen that the inductance rate is an important factor for the output torque, so Table 2 shows the inductance rates of both SRMs. The inductance rate can be calculated as:

$$\frac{dL(\theta,i)}{d\theta} = \frac{L_{Max} - L_{Min}}{\theta} \tag{2}$$

in which, d$L(\theta, i)$/dθ is the inductance rate, L_{max} is the maximum inductance, L_{min} is the minimum inductance and θ is the rotor position between maximum and minimum inductance. For the conventional and segmental 12/8 structures, there is 22.5 degree between maximum and minimum inductance.

Table 2 shows the inductance rates of both SRMs for 110-Ampere excitation current (full-load). From this Table, it can be seen that the inductance rate of segmental SRM is 0.0033 mH/deg, while the inductance rate of conventional SRM is only 0.0028 mH/deg. The inductance rates imply

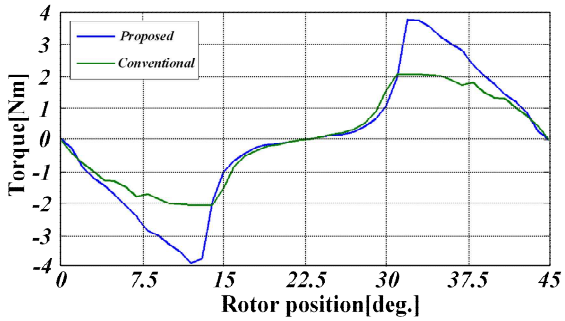

Fig. 10. Torque characteristics of conventional and segmental type SRMs

that the segmental SRM can offer better performance in terms of the torque production.

3.1.3 Torque characteristics

Fig. 10 shows the torque comparison of the conventional and segmental rotor type 12/8 SRMs. Both conventional and segmental rotor types use the same dimension and input parameters. As shown in Fig. 8, the average torque of conventional type is 1.778 Nm, while segmental rotor type is 2.011 Nm. The average torque of the segmental rotor type is 13.1% higher than that of the conventional one.

The electromagnetic behavior of each motor phase is commonly analyzed independently, since the magnetic interactions between phases are typically very small for conventional motors and can be ignored for simplicity reason. However, in this case, in order to analyze the torque ripple of conventional and segmental types, the continuous torque of both types are required.

Figs. 11 and 12 show the continuous torque of both types, respectively. From the figures, it can be seen that the maximum torque produced by 110A-excitation current of conventional and segmental types are 2.12 Nm and 3.81 Nm. The continuous torque is based on the neutral commutation angle (22.5 mechanical degrees), with no overlap among the phase.

However, to achieve low torque ripple, usually there is an overlap between phases in the overlapping region, both phases contribute torque production to the machine. Also, the torque ripple can be optimized by regulating the turn on and off angles to make the motor torque ripple lower, while the optimal control method to reduce the torque ripple is not discussed in this paper.

Table 3 shows the torque ripple comparison of the conventional and segmental type SRMs. In Table 3, the torque ripple of the motor can be calculated as,

$$k_r = \frac{T_{Max} - T_{Min}}{T_{Ave}} \times 100\% \quad (3)$$

in which, k_r is the torque ripple of the motor, T_{max}, T_{min} and T_{ave} is the maximum torque, minimum torque and average torque, respectively. The torque ripple of segmental SRM

Table 3. Torque ripple comparison of the conventional and segmental type SRMs

Motor type	10A	30A	50A	70A	90A	110A
Conventional type (%)	87.0	82.0	82.0	86.9	93.2	95.7
Segmental type (%)	138.1	138.9	137.3	127.8	118.0	111.4

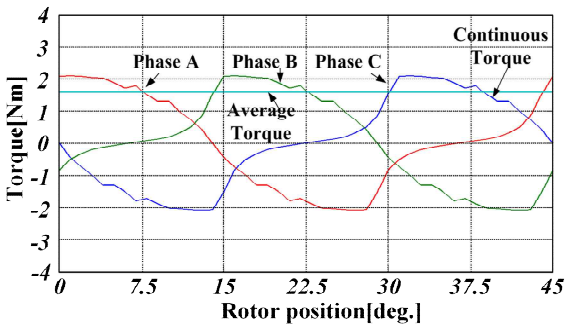

Fig. 11. Continuous torque of conventional type

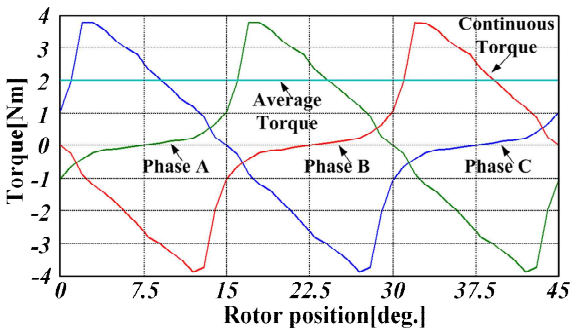

Fig. 12. Continuous torque of segmental rotor type

is higher than that of conventional one.

Fig. 13 shows the torque profiles of conventional and segmental rotor types, respectively.

Fig. 14 shows the comparison of simulated average torque for different current levels. As shown in Fig. 13, the segmental type has higher average torque than that of conventional type at all current levels. However, the superiority becomes smaller and smaller with current increase. It is because the segmental structure is easier to get saturated than the conventional type as shown in Fig. 8.

3.2. Dynamic Characteristics

In order to further compare the performances of conventional and segmental SRMs, dynamic analysis is executed.

3.2.1. Asymmetric converter

Due to many advantages, such as the capability of independent control for each phase and four switching

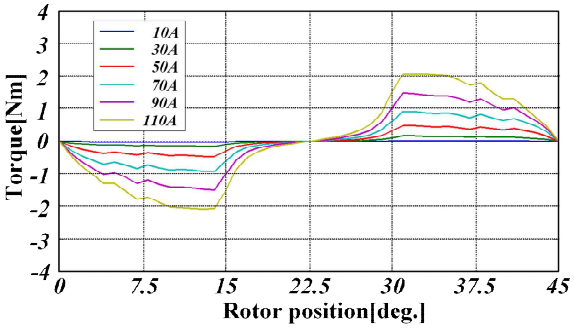

(a) Conventional type

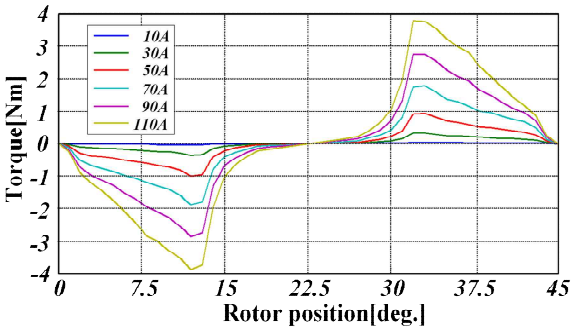

(b) Segmental type

Fig. 13. Torque profiles at all current levels

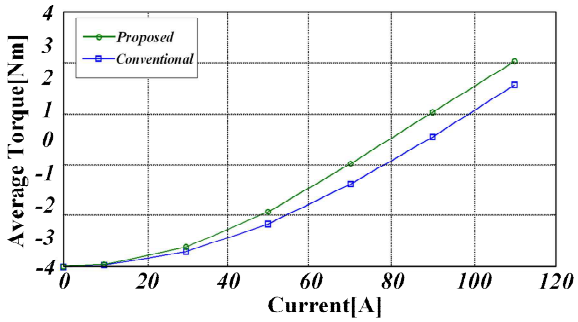

Fig. 14. Average torque versus current

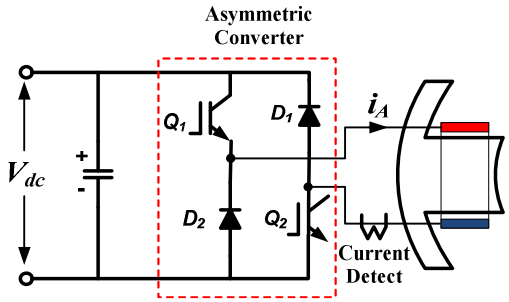

Fig. 15. Topology of asymmetric converter

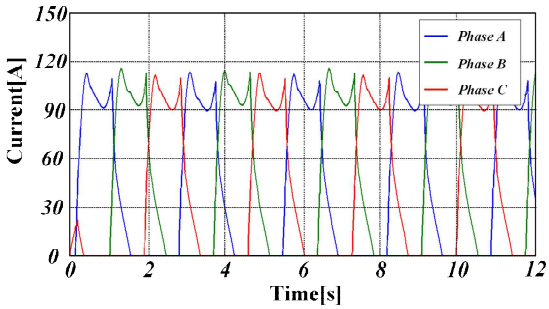

(a) Conventional SRM

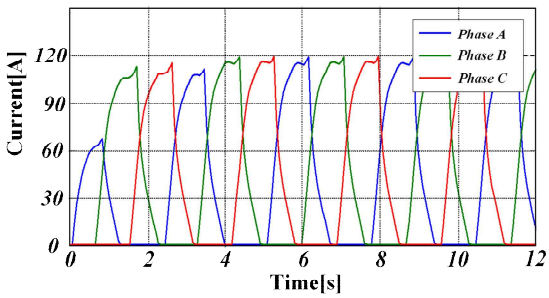

(b) Segmental SRM

Fig. 16. Current profiles at rated condition

modes, asymmetric converters are adopted for conventional and segmental type. Fig. 15 shows the topology of the asymmetric converter circuit.

3.2.2. Simulation results

An external circuit is built and both of motors are simulated with the same external circuit at rated condition.

Meanwhile, full voltage control method is used to control the both motor types. For the conventional SRM, the turn on and off angle are 2.4° and 18.4°, respectively, while for the segmental SRM, the angles are 0° and 16.5°, respectively.

Fig. 16 shows the transient currents in the two motors. From the figures, it can be seen that the peak value of currents in conventional SRM is about 110A, while it is about 105A for the segmental motor. Furthermore, at the end of the conduction cycle, the current has an upward peak, which is caused by the saturation of the core. It can be optimized by regulating the turn on and off angles to increase motor efficiency, while the optimal control method to improve efficiency is not discussed in this paper.

Fig. 17 shows the core loss of the two motor types when they are operating at rated condition. Compared with Fig. 17 (a) and (b), it can be seen that the core losses are mainly produced at commutation region. Furthermore, the core loss is non-uniform in the conventional type, while it is uniform in the segmental type, as explained in section Ⅱ.

Fig. 18 shows the basic control scheme for both SRMs. In this application, the speed control was applied. The motor speed is measured by the encoder and estimator module. The motor speed feeds the PI control module. The motor speed ω is compared to the reference speed ω*. The output of the PI module is PWM duty cycle. The output of the PI regulator is the input of the PWM generator module, which will generate PWM signals to operate the inverter.

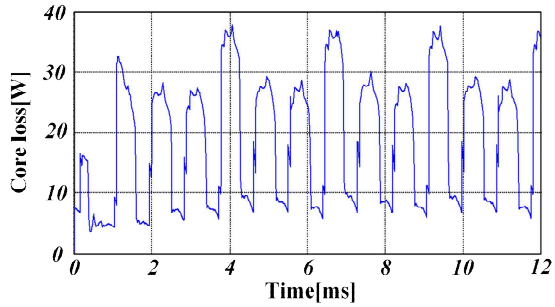

(a) Conventional SRM

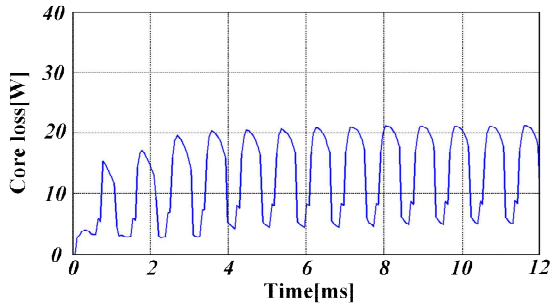

(b) Segmental SRM

Fig. 17. Core loss profiles at rated condition

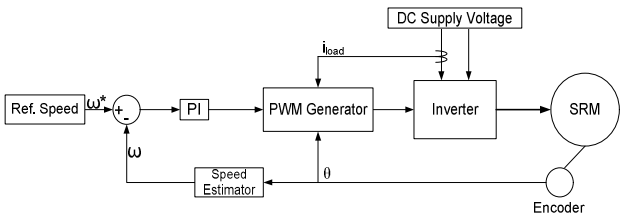

Fig. 18. Control scheme for conventional and segmental

Depend on the rotor position signal that is fed by encoder, the phases of the motor will be excited alternately. The load current measured by a current sensor will be fed to PWM generator module to protect the drive system. When the load current is greater than limited current, the PWM signals will be turned off to protect the drive system. In this application, the current control was not applied. Only one current sensor was used to measure the load current.

The prototype machines have been subjected to dynamic performance testing. Fig. 18 shows the experimental platform. As shown in Fig. 18, the machines have been coupled with a dynamometer and driven by a three-phase asymmetric inverter. The experiments are realized by a Texas Instruments (TI) TMS320F28335 digital signal processor (DSP). The output power is measured by a 2WB43 dynamometer and the input power is measured by the PPA2530 power analyzer.

Table 4 shows the steady-state characteristics of FEM analysis and experiment results. The calculating method for the data in Table 4 is given in Appendix. From Table 4, it can be seen that the FEM and experimental results have some errors. It will be explained as follow:

Table 4. Steady-state characteristics of both SRMs

Parameter	Conventional		Segmental	
	FEM	Exp.	FEM	Exp.
Rated voltage (V)	11.34	11.26	11.28	11.16
Rated speed (rpm)	2800	2800	2800	2800
Rated torque (Nm)	1.7	1.7	1.7	1.7
Phase current – RMS (A)	60.35	63.78	57.96	61.49
Mechanical loss (W)	12.50	23.31	12.50	19.06
Copper loss (W)	76.48	85.42	70.55	79.41
Core loss (W)	20.81	28.12	16.08	21.03
Output power (W)	497.12	499.31	496.24	499.05
Input Power (W)	606.91	636.16	595.37	618.55
Efficiency (%)	81.91	78.49	83.35	80.68

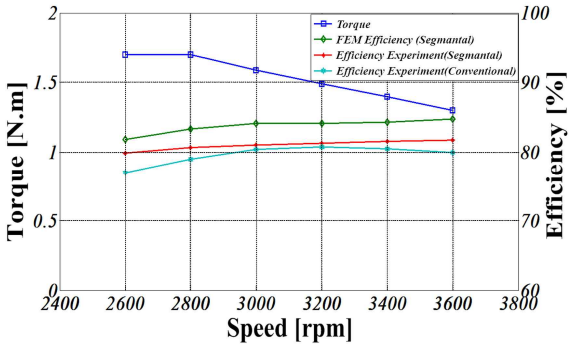

Fig. 19. Efficiency comparisons of conventional and segmental type SRMs

a) For the mechanical loss error, it is mainly caused by the estimation error. It is well known that the mechanical loss in FEM cannot be accurately calculated and it only depends on the experience of predecessors. In this paper, it is only adopted as 2.5% of rated output power. However, it is larger in the real prototype.
b) For the core loss error, it can be mainly attributable to inexact B-H characteristics provided by the steel manufactures.
c) For the copper loss and efficiency, they are mainly caused by the cumulative error, such as the error in mechanical loss and core loss.

Furthermore, it can be seen from the experiment results that the total efficiency of the motor driver system at rated condition, including the power converter and motor, is 78.49% and 80.68%, respectively. For the efficiency at other speeds, they are given in Fig. 19.

Therefore, it can be seen from Table 4 and Fig. 19 that the proposed structure could get higher efficiency than that of conventional structure at all speeds. This verifies the validity of the proposed structure.

4. Conclusion

Performance comparisons of switched reluctance motor for cooling fan application are dealt in this paper.

Conventional and novel segmental type motors with the same dimension are compared. The torque and torque ripple are also compared and the segmental structure offers better performance in terms of the maximum and average torque, while the torque ripple of conventional type is smaller than segmental type. Furthermore, in the FEM and experiment, the segmental structure decreases the core losses because of the short flux and no flux reversal in the stator, which leads to higher efficiency.

Appendix

The parameters in TABLE 4 are calculated as follows：

1) Copper Loss

The copper loss is proportional to the square of the phase RMS current and phase winding resistance. Hence, according to the current waveform, the copper loss can be calculated as,

$$P_{cu} = mI_{phrms}^2 R_{ph} \tag{4}$$

$$I_{phrms} = \sqrt{\frac{1}{T}\int_0^T I_m^2 dt} \tag{5}$$

where, m is the number of phase, I_{phrms} is the RMS current of phase, R_{ph} is the phase resistance, T is the time of one period, I_m is the phase current. For the phase resistance of conventional and segmental rotor type SRM, please refer to Table 1. Furthermore, the phase current in FEM is calculated based on Fig. 14, while it is directly measured by a current sensor in the experiments.

2) Windage and Friction Loss

For simulation, the mechanical losses Pm can be estimated as 2~3% of rated output power. In this paper, 2.5% is adopted. Nevertheless, the actual losses are measured in the experiment.

3) Core Loss

The core loss is composed of hysteresis loss, excessive loss, and eddy-current loss. It can be calculated as,

$$P_{losses} = P_h + P_c + P_e \tag{6}$$

$$P_h = k_h f\left(B_m\right)^2 \tag{7}$$

$$P_e = k_e\left(fB_m\right)^{1.5} \tag{8}$$

$$P_c = k_c\left(fB_m\right)^2 \tag{9}$$

in which, Ph, Pe, Pc are the hysteresis loss, excessive loss, and eddy-current loss, respectively; kh, ke and kc are the coefficient of hysteresis loss, excessive loss, and eddy-current loss, respectively. In the analysis, S18 is used as the stator and rotor material. From the datasheet, kh, ke and kc are given as 270.39764, 4.30046 and 0.30463 W/m3, respectively.

For experiment, the core loss can be derived as,

$$P_c = P_{input} - P_{output} - P_m - P_{cu} \tag{10}$$

where, Pinput and Poutput are the input and output power, respectively.

Acknowledgment

This work was supported by “Human Resources Program in Energy Technology” of the Korea Institute of Energy Technology Evaluation and Planning(KETEP), granted financial resource from the Ministry of Trade, Industry & Energy, Republic of Korea (No. 20164010200940)

References

[1] D. H. Lee, Z. G. Lee, J. Liang, J. W. Ahn, “Single-phase SRM drive with torque ripple reduction and power factor correction,” *IEEE Transaction on Industry Applications*, vol. 43, no. 6, pp. 1578-1587, Nov.-Dec. 2007.

[2] D. H. Lee and J. W. Ahn, “Design and analysis of hybrid stator bearingless SRM,*” J. Elect. Eng. Technol.*, vol. 6, no. 1, pp. 94-103, Jan. 2011.

[3] D. H. Lee, J. H. Pham and J. W. Ahn, “Design and operation characteristics of four-two pole high-speed SRM for torque ripple reduction,” *IEEE Transaction on Industrial Electronics*, vol. 60, no. 9, pp. 3637-3643, Sep. 2013.

[4] S. M. Yang, J. Y. Chen, “Controlled dynamic braking for switched reluctance motor Drives with a rectifier front end,” *IEEE Transactions on Industrial Electronics*, vol.60, no.11, pp. 4913 - 4919, 2013.

[5] B. Bilgin, A. Emadi, M. Krishnamurthy, “Comprehensive evaluation of the dynamic performance of a 6/10 SRM for traction application in PHEVs,” *IEEE Transactions on Industrial Electronics*, vol. 60, no. 7, pp. 2564 - 2575, 2013

[6] B. Bilgin, A. Emadi, M. Krishnamurthy, “Design considerations for switched reluctance machines with a higher number of rotor poles,” *IEEE Transactions on Industrial Electronics*, vol. 59, no. 10, pp. 3745-3756, 2012

[7] B.C. Mecrow, “New winding configurations for doubly salient reluctance machines,” *IEEE Transaction on Industry Applications*, vol. 32, no. 6, pp. 1348-1356, Nov.-Dec. 1996.

[8] J. Oyama, T. Higuchi, T. Abe, and K. Tanaka, “The fundamental characteristics of novel switched reluctance motor with segment core embedded in aluminum rotor block,” *Journal of Electrical Engineering & Technology*, vol. 1, no. 1, pp. 58-62,

2006.
[9] T. Higuchi, K. Suenaga, T. Abe, "Torque ripple r eduction of novel segment type switched reluctan ce motor by increasing phase number", *in Procee ding International Conference on Electrical Mach ine and Systems* (*ICEMS 2009*), 2009.
[10] C. W. Lee, R. Krishnan, N. S. Lobo, "Novel Two-p hase Switched Reluctance Machine using Commo n-Pole E-Core Structure: Concept, Analysis, and Experimental Verification" Industry Applications C onference, 2007. 42nd IAS Annual Meeting.

Kwang-Il Jeong was born in Jinju, Korea in 1986. He received his B.S degree in Mechatronics Engineering from Gyeongnam National University of Science and Technology, Jinju, Korea, in 2009, and M.S degree in Kyungsung University, Busan, Korea, in 2012. Now, he is studying in Kyungsung University, Busan, Korea as a Ph.D. student in the Department of Mechatronics Engineering. His research interests are motor design and control.

Zhenyao Xu (S'14) was born in Dalian, China, in 1987. He received the B.S. and M.S. degrees in electrical engineering from Shenyang University of Technology, Shenyang, China, in 2009 and 2012, respectively, and the M.S. and Ph.D degrees in mechatronics engineering from Kyungsung University, Busan, Korea, in 2012 and 2016, respectively, From 2016 to 2017, he was an Assistant Professor in mechatronics engineering from Kyungsung University, Busan, Korea. Since 2017, he has been an Assistant Professor in Department of Space Automation Technologies & Systems, Shenyang Institute of Automation, the Chinese Academy of Sciences, Shenyang, China. His research interests include motor design and motor control systems.

Dong-Hee Lee was born on Nov. 11, 1970 and received his B.S, M.S., and Ph. D degrees in Electrical Engineering from Pusan National University, Pusan, Korea in 1996, 1998, and 2001, respectively. He worked as a Senior Researcher of Servo R&D Team at OTIS-LG, from 2002 to 2005. He has been with Kyungsung University, Pusan, Korea as an Assistant professor in the Department of Mechatronics Engineering since 2005. He has been the Director of the Advance Electric Machinery and Power Electronics Center since 2009. His major research field is Power Electronics and motor control system.

Jin-Woo Ahn was born in Busan, Korea, in 1958. He received his B.S., M.S., and Ph.D. degrees in Electrical Engineering from Pusan National University, Busan, Korea, in 1984, 1986 and 1992, respectively. He has been with Kyungsung University, Busan, Korea, as a professor in the Department of Mechatronics Engineering since 1992. He is Vice President of KIEE and the director of the Smart Mechatronics Advanced Research and Technology Institute and Senior Easy Life RIS Center. He is the author of five books including SRM, the author of more than 200 papers and has more than 30 patents. His current research interests are advanced motor drive systems and electric vehicle drives. He also received many awards from IEEE, KIEE and KIPE and including Order of Science and Technology Merit from the President of the Republic of Korea for his numerous contributions for the electrical engineering. He served as a Conference Chairman of International Conference on Electric Machines and Systems2013 (ICEMS 2013), and of International Conference on Industrial Technology 2014 (IEEE/ICIT2014) and serving as a Conference Chairman of IEEE Transportation Electrification Conference and Expo 2016 Busan (ITEC2016 Busan). He is a Fellow of the Korean Institute of Electrical Engineers, a member of the Korean Institute of Power Electronics and a Senior member of the IEEE.